The influence of film thickness on photovoltaic effect for the $Fe_3O_4/SrTiO_3$:Nb heterojunctions

2010 J. Phys. D: Appl. Phys. 43 205004

(http://iopscience.iop.org/0022-3727/43/20/205004)

IOP PUBLISHING JOURNAL OF PHYSICS D: APPLIED PHYSICS

J. Phys. D: Appl. Phys. **43** (2010) 205004 (5pp) doi:10.1088/0022-3727/43/20/205004

The influence of film thickness on photovoltaic effect for the $Fe_3O_4/SrTiO_3$:Nb heterojunctions

A D Wei, J R Sun[1], Y Z Chen, W M Lü and B G Shen

Beijing National Laboratory for Condensed Matter Physics and Institute of Physics, Chinese Academy of Sciences, Beijing 100190, People's Republic of China

E-mail: jrsun@g203.iphy.ac.cn

Received 19 March 2010, in final form 20 April 2010
Published 6 May 2010
Online at stacks.iop.org/JPhysD/43/205004

Abstract

Fe_3O_4 films with the thickness ranging from 5 to 160 nm have been grown on $SrTiO_3$: Nb (0.05wt%) substrates by the pulsed laser deposition technique. The good quality of the Fe_3O_4 film was confirmed by x-ray diffraction and magnetic analyses. It is found that the interfacial barrier of the resultant junctions, determined by the photovoltaic technique, decreases as film thickness increases from ∼5 to ∼40 nm, with a relative change of ∼20%, and saturates at a value of ∼1.2 eV above the thickness of 40 nm. Variation of lattice strains in the Fe_3O_4 film may be the reason for the thickness dependence of the interfacial barrier.

(Some figures in this article are in colour only in the electronic version)

1. Introduction

As a half metal, Fe_3O_4 has received considerable attention in the past few decades [1–3]. It has been theoretically predicted to be fully spin polarized [4, 5]. The practical spin polarization is higher than ∼80%, as experimentally proved [2, 3, 6]. As a result, it is usually used in various artificial structures that are designed based on the transport process of spin polarized electrons, such as magnetic tunnelling junctions and the heterostructures for spin injection.

It is obvious that the properties of the manganite-based devices depend crucially on the interfacial state. In general, the interfacial state of the material is different from that of the bulk, due to the effect of strains and defects, and degenerated interfacial properties, for example reduced spin polarization [2], are usually the result. It is therefore highly desirable to get a control on the interfacial state as film thickness, interfacial strains and structural defects vary, which is helpful for the design of artificial materials/devices. In this paper, we show the influence of film thickness on the interfacial state of the $Fe_3O_4/SrTiO_3$: Nb junctions, as demonstrated by the variation of the interfacial barrier. The photovoltaic technique has been used for the determination of the interfacial barrier, to avoid the difficulties encountered by the analyses of the current–voltage and capacitance–voltage relations when electron tunnelling occurs in the junction. A significant decrease in interfacial potential was observed as film thickness increases. This effect has been ascribed to the relaxation of compressive strains as film thickness increases.

2. Experiments

Two series of Fe_3O_4-based Schottky junctions were fabricated by depositing Fe_3O_4 films on 0.05wt% Nb-doped (0 0 1) $SrTiO_3$ (STON) substrates using the pulsed laser ablation technique. The wavelength of the laser is 248 nm, the repetition rate is 5 Hz, and the flux is 4 J cm^{-2} for the first series of samples and 6 J cm^{-2} for the second series of samples. During the deposition, the substrate temperature was kept at 500 °C and 550 °C for the first and second series of junctions, respectively, and the oxygen pressure was 4×10^{-3} Pa. The film thickness (t) varies between 5 and 160 nm, controlled by deposition time.

The surface morphology and magnetic microstructure of the films were analysed by atomic force microscopy (AFM) and magnetic force microscopy (MFM), respectively. Magnetic measurement was performed on a quantum design superconducting quantum interference device magnetometer.

[1] Author to whom any correspondence should be addressed.

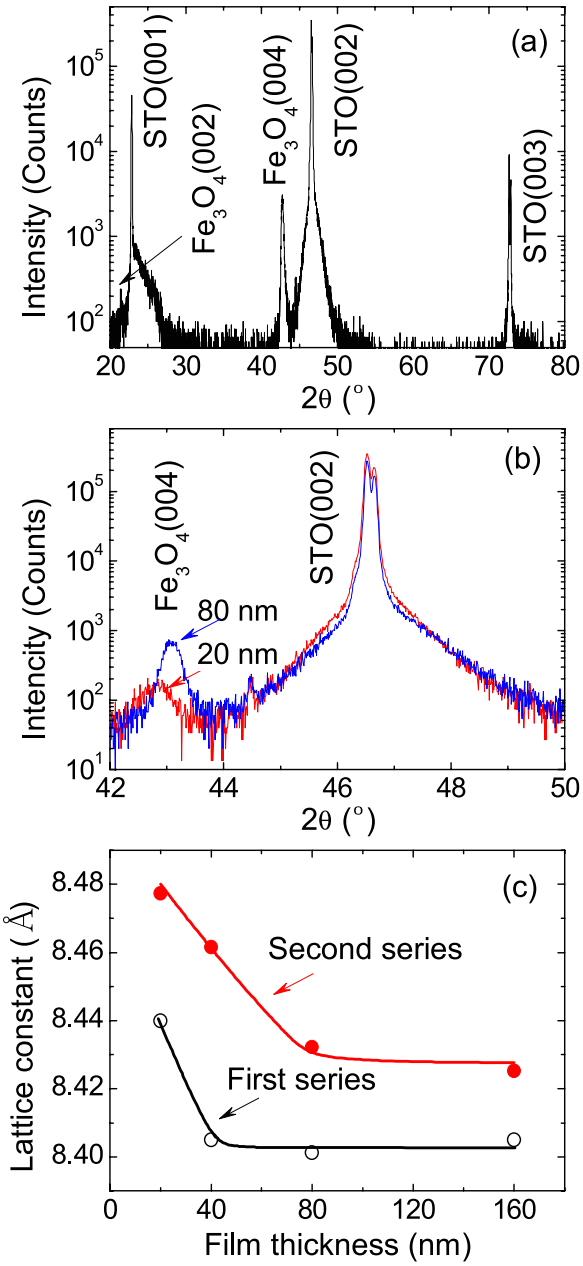

Figure 1. (*a*) X-ray spectra of the Fe_3O_4 films. (*b*) A close view of the (0 0 4) peak. (*c*) Out-of-plane lattice constant as a function of film thickness. Black hollow circle for the first series, and red solid circle for the second series. Solid lines are a guide to the eye.

3. Results and discussions

The epitaxial growth of the Fe_3O_4 film was confirmed by x-ray diffraction (XRD) analysis. All the films are highly oriented, as demonstrated by the appearance of the (0 0 l) peaks and the absence of any other reflections of different orientations (figure 1(*a*), indexed based on cubic structure). Figure 1(*b*) is an amplified view of the (0 0 4) peak. It shows a gradual high angle shift as film thickness increases, signifying a decrease in the out-of-plane lattice constant (*c*). For the first series junctions, as shown by figure 1(*c*), the lattice parameter decreases rapidly from ∼8.44 to ∼8.40 Å as film thickness increases from ∼20 to ∼40 nm and saturates at ∼8.40 Å above 40 nm. For the second series samples, significant changes occur in the thickness range below ∼60 nm, and the maximal variation $\Delta c/c$ is ∼0.6%. The XRD peaks of the Fe_3O_4 films are invisible when film thickness is below 10 nm. The difference in lattice constants for the two sets of samples could be ascribed to the different preparation conditions.

Due to the considerable lattice mismatch between Fe_3O_4 and STON [$(8.398-2\times3.901)/8.398 = 7.6\%$)], compressive strains are present in the films. The decrease in *c* is a consequence of lattice relaxation as film thickness increases. From figure 1(*c*) it is obvious that the most significant lattice relaxation occurs in the films with a thickness below ∼60 nm. This is somewhat different from the manganite films, for which substantial lattice relaxation occurs below the thickness of ∼20 nm [7, 8]. Meanwhile, the maximal relative lattice constant change in the Fe_3O_4 film is also smaller than that in the manganite film (∼0.6% versus ∼1.8%). These may indicate a poor coherent growth of the Fe_3O_4 film on the STON substrate, due to the large lattice mismatch.

Figures 2(*a*) and (*b*) show the surface morphology and the MFM image of the Fe_3O_4 film, respectively. The film is fairly smooth. The root-mean-square roughness is ∼1.2 nm for the film of 80 nm, and it decreases as film thickness decreases. The average grain size is ∼7 nm for the film of 80 nm, and it grows with film thickness. Randomly distributed magnetic domains were detected by the MFM, aligning in the normal direction of the film plane, which confirms the long-range ferromagnetic order in the Fe_3O_4 film. Figure 2(*c*) shows the hysteretic loop of the Fe_3O_4 film measured at 300 K (80 nm). The magnetization is ∼320 emu cm^{-3} under the field of 2 T, comparable to the expected magnetization (∼471 emu cm^{-3}) [9]. No saturation is reached up to the field of 5 T, probably indicating the presence of antiphase boundaries near the Fe_3O_4–STON interface [10]. The coercive field is ∼0.05 T and the remanence is ∼210 emu cm^{-3}. These are the typical properties of Fe_3O_4 as reported in [11], and show the good quality of our Fe_3O_4 films.

All the junctions, even the ones composed of ultra-thin films, exhibit a fairly rectifying behaviour (not shown). A careful analysis of the current (*I*)–voltage (*V*) characteristics, however, indicates the presence of considerable leakage current when bias voltage is low and the parallelism of the log *I*–*V* curves recorded under different temperature (see [3]). The latter is a signature of electron tunnelling, which prevents an accurate determination of the interfacial barrier based on the *I*–*V* curves. It is fortunate that neither the leakage process nor the tunnelling process will affect the photovoltaic effects (PVEs) of the junction considering the fact that the PVE is exclusively determined by the interfacial barrier. In the following we will try to obtain the interfacial potential based on the data of the PVE. As we know, electrons in the Fe_3O_4 electrode can be excited by photons with the energy of $h\nu$ when the condition $\Phi_B \leqslant h\nu$ is satisfied, and the extra charge carriers can penetrate through the junction region under the driving of the built-in electric field, yielding a photocurrent, where *h* is the Planck constant, ν is the frequency of the photon and Φ_B is the height of the energy barrier in the Fe_3O_4/STON junction. It is obvious that the higher the photon energy is, the

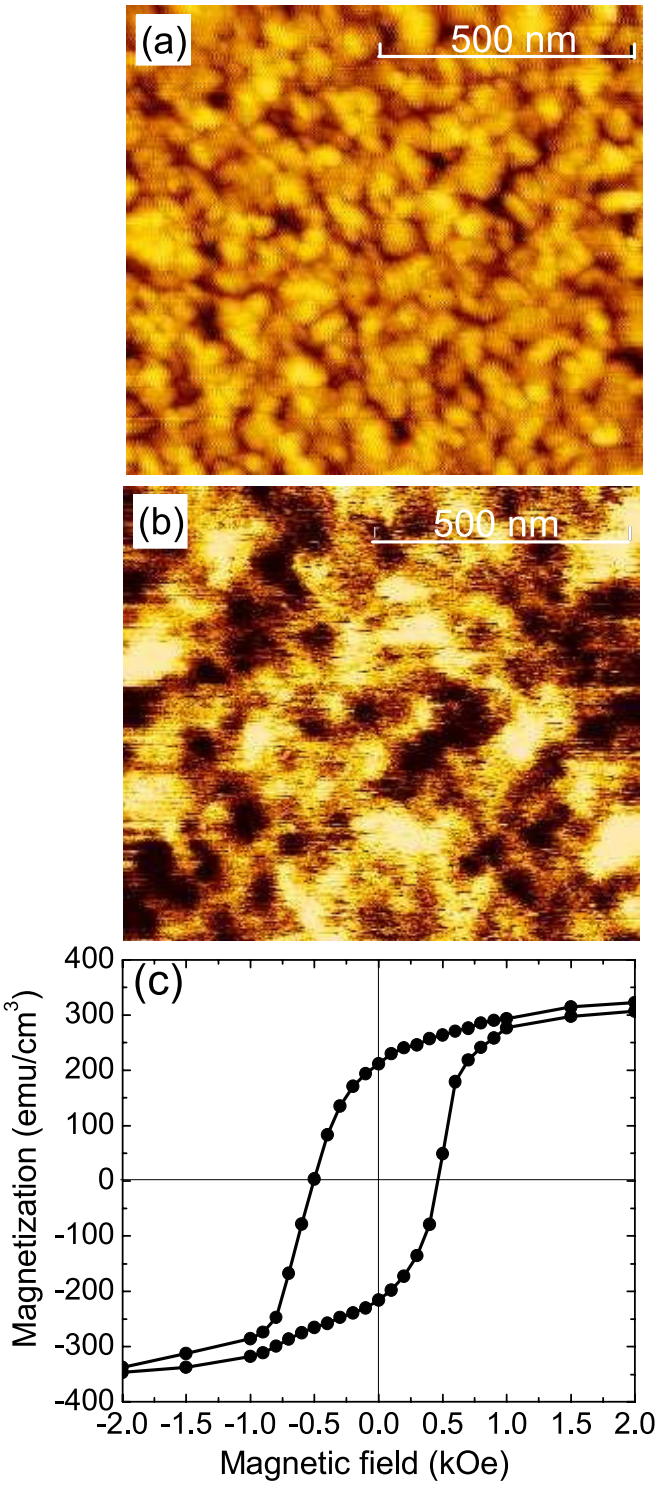

Figure 2. Typical AFM (*a*) and MFM (*b*) images for the Fe_3O_4 film of 80 nm in thickness ($1 \times 1\ \mu m^2$). (*c*) The hysteretic loop of the Fe_3O_4 film of 80 nm, with the magnetic field being applied along the film plane.

stronger the PVE will be. There is a simple relation between the quantum efficiency, proportional to the number of excited electrons by each photon, and photon energy [12].

$$R \propto (h\nu - \Phi_B)^2 \qquad (1)$$

when $|h\nu - \Phi_B| \geqslant 3k_BT$, where k_B is the Boltzmannn constant and R is the quantum efficiency. Based on this relation the interfacial barrier can be experimentally determined. This is an effective approach that avoids the difficulty of deducing Φ_B from the I–V characteristics that deviate from the thermionic emission process.

Lasers with wavelengths between 530 and 1000 nm were used in the present experiment. The spot size of the incident light is ~1 mm in diameter. Photocurrent was recorded during the light illumination, as a function of wavelength. Take the first series samples as a representative. Figures 3(*a*) and (*b*) show the photocurrents produced by the lights of 532 nm and 660 nm, respectively. The photocurrent shows a sudden jump when the shutter of the light is opened, and stays at this value until the light is closed. The photocurrent decreases as wavelength increases, indicating less efficiency of the long wavelength light. The typical photocurrent is ~6.3 nA mW^{-1}, for the lights of 532 nm, and ~0.9 nA mW^{-1}, for the wavelength of 660 nm, and there is no significant photocurrent detected when the wavelength exceeds 980 nm. This result actually implies the presence of an interfacial barrier, and only the photons with energy well above Φ_B are effective. The photocurrent is generally high in thin Fe_3O_4 films. In contrast to thick films, the photocurrent of the thin films shows a relatively sluggish response to light illumination, instead of a steep jump as expected. This feature is usually observed in the junctions with significant leakage current, and could be ascribed to the time-delay of a R–C circuit, where R and C are the resistance and capacitance of the junction, respectively. Essentially similar results are obtained for the second set of samples.

Based on the data in figure 3, the quantum efficiency, R, which is proportional to the photocurrent produced by each photon, can be deduced. Figure 4 presents the $R^{1/2}$–$h\nu$ relations obtained for the first series of samples. Similar results are obtained for the second series junctions. The $R^{1/2}$–$h\nu$ relation is well linear for all samples, which indicates the presence of a definite interfacial barrier in the junction. As film thickness increases from 5 to 40 nm, the $R^{1/2}$–$h\nu$ curve exhibits an obvious left shift along the $h\nu$ axis, in addition to the change in the $R^{1/2}$–$h\nu$ slope. This means a growth of interfacial barrier as film thickness decreases. When the film thickness exceeds 40 nm, no significant change in the intercept for the $R^{1/2}$–$h\nu$ curve is observed.

Interfacial barrier as a function of film thickness is shown in figure 5. Similar results are obtained for the two series of samples. The height of the interfacial barrier of thin film (<40 nm) junctions is obviously larger than that of thick film (>40 nm) junctions. For the first series junctions, Φ_B decreases rapidly from 1.46 to 1.2 eV as t increases from 5 to 20 nm, with a total change in $\Delta\Phi_B \approx 0.26$ eV. For the second series junctions, Φ_B decreases rapidly from 1.43 to 1.2 eV as t increases from 10 to 20 nm, with a total change in $\Delta\Phi_B \approx 0.23$ eV. The relative change is ~20% for the two series junctions. Comparing the data in figures 1(*b*) and 5, we found that the interfacial barrier and lattice constant exhibit a synchronous variation with film thickness. This behaviour is similar to what happened in the $La_{0.67}Ca_{0.33}MnO_3$/STON junctions [13].

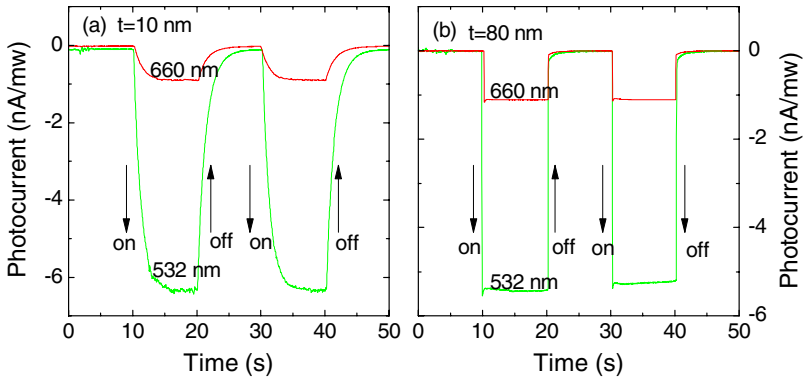

Figure 3. Typical photocurrent of the first series Fe_3O_4/STON junctions with the film thicknesses of 10 nm (*a*) and 80 nm (*b*). Arrows indicate the times for the light on and off.

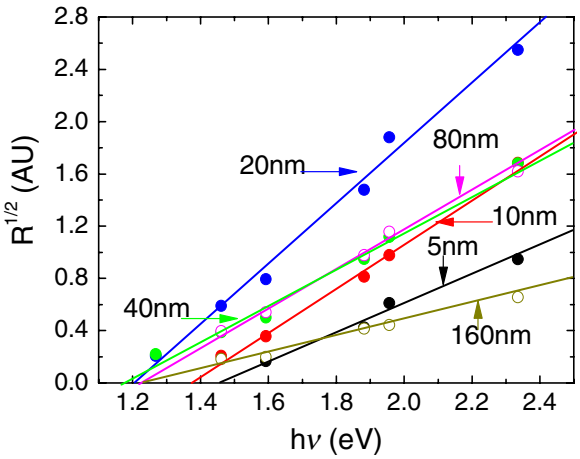

Figure 4. Square root quantum efficiency as a function of photon energy for the first series of Fe_3O_4/STON junctions. Solid lines are a guide to the eye.

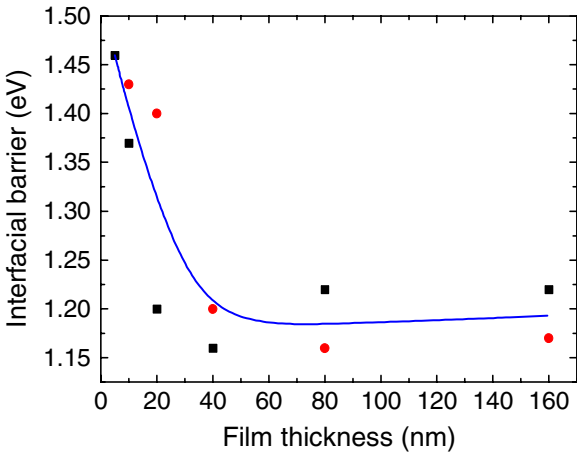

Figure 5. Interfacial barrier as a function of the film thickness. Solid and hollow symbols represent the results of the first and the second series of samples, respectively.

A further analysis reveals the difference between the strain effects in $La_{0.67}Ca_{0.33}MnO_3$/STON and Fe_3O_4/STON. With the relaxation of the lattice strain, the interfacial barrier grows in the former whereas it reduces in the latter. As is well known, the lattice strain is tensile in the $La_{0.67}Ca_{0.33}MnO_3$ films and compressive in the Fe_3O_4 films. It is clear that the Φ_B increases or decreases when the film is in a compressive or tensile state. Therefore, the results obtained for $La_{0.67}Ca_{0.33}MnO_3$/STON and Fe_3O_4/STON depict a complete picture for the strain effect on interfacial barrier in oxide junctions.

The change in Φ_B with lattice strains actually implies a change in the Fermi level of Fe_3O_4 considering the fact that strain in Fe_3O_4 will generally not affect STON. This work therefore suggests a reduction/growth in the Fermi level in a tensile/compressive oxide film, and the typical change is 0.1–0.2 eV. This conclusion could be generic noting the significant difference of the manganite and magnetite. In fact, Fix *et al* have reported a change in the energy band of the Sr_2FeMnO_6 films that are in a compressive state, characterized by the increase in the band gap of the majority spin states from ∼0.53 to ∼0.36 eV as the compressive strains in the film develop [14]. Similar processes may occur in the Fe_3O_4 films.

How such a large change in the Fermi level is induced by lattice strain is not very clear at present. It has been proposed that the spin state of Fe^{2+} may experience a high to intermediate transition under high pressure [15]. The Fermi level in this case could be low considering the enhancement of the interaction between the positive core and d-electrons. Noting the presence of significant compression in ultra-thin Fe_3O_4 films, the interfacial barrier in the corresponding junctions may be larger than that in the junctions composed of thick films. Obviously, this is a preliminary explanation, and further work is required for a thorough understanding of the strain effect.

4. Summary

Fe_3O_4 films with thicknesses ranging from 5 to 160 nm have been grown on $SrTiO_3$: Nb (0.05wt%) substrates by the pulsed laser deposition technique, and strain effects on the corresponding junctions have been studied. The good quality of the Fe_3O_4 film was confirmed by XRD and magnetic analyses. It is found that the interfacial barrier of the resultant junctions, determined by the photovoltaic technique, decreases as the film thickness increases from ∼5 to ∼40 nm, with a relative change of ∼20%, and saturates at a value of ∼1.2 eV above the thickness of 40 nm. Variation of lattice strains in the Fe_3O_4 film is assumed to be the reason for the thickness

dependence of the interfacial barrier. Possible origins for the change in the Fermi level of the Fe_3O_4 films in different strain states are discussed. This work could be important for the designing of artificial heterostructures.

Acknowledgments

The authors are grateful to Dr Q L Ma for measurement of the thickness of the films. This work has been supported by the National Basic Research of China, the National Natural Science Foundation of China, the Knowledge Innovation Project of the Chinese Academy of Science and the Beijing Municipal Nature Science Foundation.

References

[1] Margulies D T, Parker F T, Rudee M L, Spada F E, Chapman J N, Aitchison P R and Berkowitz A E 1997 *Phys. Rev. Lett.* **79** 5162
[2] Kundaliya D C, Ogale S B, Fu L F, Welz S J, Higgins J S, Langham G, Dhar S, Browning N D and Venkatesan T 2006 *J. Appl. Phys.* **99** 08K304
[3] Chen Y Z, Sun J R, Xie Y W, Wang D J, Lu W M, Liang S and Shen B G 2007 *Appl. Phys. Lett.* **90** 143508
[4] Yanase A and Siratori K 1984 *J. Phys. Soc. Japan* **53** 312
[5] Zhang Z and Satpathy S 1991 *Phys. Rev.* B **44** 13319
[6] Ziese M, Köhler U, Bollero A, Höhne R and Esquinazi P 2005 *Phys. Rev.* B **71** 180406
[7] Orgiani P, Petrov A Y, Adamo C, Aruta C, Barone C, De Luca G M, Galdi A, Polichetti M, Zola D and Maritato L 2006 *Phys. Rev.* B **74** 134419
[8] Jin S, Gao G, Wu W and Zhou X 2007 *J. Phys. D: Appl. Phys.* **40** 305
[9] Margulies D T, Parker F T, Spada F E, Goldman R S, Li J, Sinclair R and Berkowitz A E 1996 *Phys. Rev.* B **53** 9175
[10] Zhou W L, Wang K-Y, O'Connor C J and Tang J 2001 *J. Appl. Phys.* **89** 7398
[11] Chen Y Z, Sun J R, Han Y N, Xie X Y, Shen J, Rong C B, He S L and Shen B G 2008 *J. Appl. Phys.* **103** 07D703
[12] Fowler R H 1931 *Phys. Rev.* **38** 45
[13] Lü W M, Wei A D, Sun J R, Chen Y Z and Shen B G 2009 *Appl. Phys. Lett.* **94** 082506
[14] Fix T, Stoeffler D, Colis S, Ulhaq C, Versini G, Vola J P, Huber F and Dinia A 2005 *J. Appl. Phys.* **98** 023712
[15] Ding Y, Haskel D, Ovchinnikov S G, Tseng Y C, Orlov Y S, Lang J C and Mao H 2008 *Phys. Rev. Lett.* **100** 045508